Metal Iodides in Polyiodide Networks—The Structural Chemistry of Complex Gold Iodides with Excess Iodine

Per H. Svensson, Jan Rosdahl, and Lars Kloo*[a]

Abstract: Theoretical calculations that compare the I_5^- ion and the $[AuI_4]^-$ ion show that they are closely related and have potential energy surface (PES) minima corresponding to an L-shaped structure. These calculations also indicate that the I_3^- and $[AuI_2]^-$ ions should be exchangeable. These results were confirmed by the synthesis of the compounds $(Et_3S)[AuI_4]\cdot 2I_2$ (**1**) and $(Me_3S)_2[AuI_4][I_3]$ (**4**), which have been characterised by X-ray diffraction, Raman and far-IR spectroscopy. The structure of **1** is made up of $[AuI_4]^-$ units coordinated by infinite zig-zag chains of I_2 molecules, and can be regarded as $[AuI_4]^-$ ions incorporated into a polyiodide network. The structure of **4** is closely related to those of the compounds of the $M_2Au_2X_6$ family (M = Cs^+, Rb^+, NH_4^+, K^+; X = Cl^-, Br^-, I^-) which consist of square-planar $[AuX_4]^-$ and linear $[AuX_2]^-$ ions. However, in the structure of **4**, the $[AuX_2]^-$ ions are replaced by I_3^- ions.

Keywords: ab initio calculations · gold · iodine · quantum-chemical calculations · structure elucidation · vibrational analysis

Introduction

Polyiodide structures can, with a few exceptions, be described as formed from three subunits: I^-, I_2 and I_3^-, which coordinate to each other by formal closed-shell interactions (I^- and I_3^- act as donors and I_2 as acceptor).[1–4] A vast range of polyiodides have been synthesised and the structures are highly dependent on the size and polarisability of the cation. At present, polyiodides with formal contents up to I_{29}^{3-} are known and many of them have found applications in areas such as electronics, fuel cells and batteries.[5–9] Recently, polyiodides have provoked interest since they are one of the few compounds that form extended anionic inorganic networks.[5, 10, 11]

The $(R_3S)I_x$ (R = Me,Et; $x = 2-11$) polyiodides have been shown to be appropriate reaction media for the study and isolation of modified polyiodide networks.[12,13] The addition of iodide acceptors or metal iodides to an $(R_3S)I_x$ melt exposes the iodine to a competition for iodide ions. This enables the insertion of guest atoms into the polyiodide networks and thus modification of the I^--donating properties becomes possible. Potentially, the knowledge about the effects on structure and physical properties caused by different guest molecules can enable the design of polyiodides with special properties.

[a] Dr. L. Kloo, Dr. P. H. Svensson, J. Rosdahl
Inorganic Chemistry 1, Lund University
P.O. Box 124, S-221 00 Lund (Sweden)
Fax: (+46) 46-222-44-39
E-mail: Lars.Kloo@inorg.lu.se

In this work we present the results from the use of complex gold iodides as guest molecules, which includes attempts to replace I_3^- with the analogous $[AuI_2]^-$ ion in polyiodide networks. Geometric optimisation and calculation of potential energy surfaces (PES) for $[AuI_4]^-$, I_5^-, $[AuI_2]^-$ and I_3^- have also been performed in order to investigate whether $[AuI_4]^-$ and $[AuI_2]^-$ are suitable guest molecules and are able to exchange polyiodides.

Results and Discussion

Theoretical studies of $[AuI_4]^-$, I_5^-, $[AuI_2]^-$ and I_3^-: Gold and iodine display remarkable chemical similarity both in species where the atoms have formal oxidation states of $-$I, $+$I and $+$III. Thus, both Au^- and I^-, linear $[AuCl_2]^-$ and $[ICl_2]^-$, and $[AuI_2]^-$ and I_3^-, as well as square-planar $[AuCl_4]^-$ and $[ICl_4]^-$ are known. The reason for this similar chemical behaviour is the subject of an ongoing study.[14]

The calculated I–I distance in I_3^- at the MP2 level is 2.991 Å, which is slightly too long compared with the experimental mean value of 2.922 Å.[14] However, the error is less than 3% and the result must be considered acceptable when the extremely shallow potential of linear deformation of I_3^- is taken into consideration.[15] The corresponding calculated frequencies of vibration are 58 (ν_2) 114 (ν_1) and 149 (ν_3) cm^{-1}; quite close to the experimentally observed frequencies of 75, 113 and 145 cm^{-1}.[16–18] The geometric optimisation of I_5^- at the MP2 level results in a V-shaped geometry (C_{2v}) which can be regarded as two I_2 molecules coordinated

  0947-6539/99/0501-0305 $ 17.50+.50/0

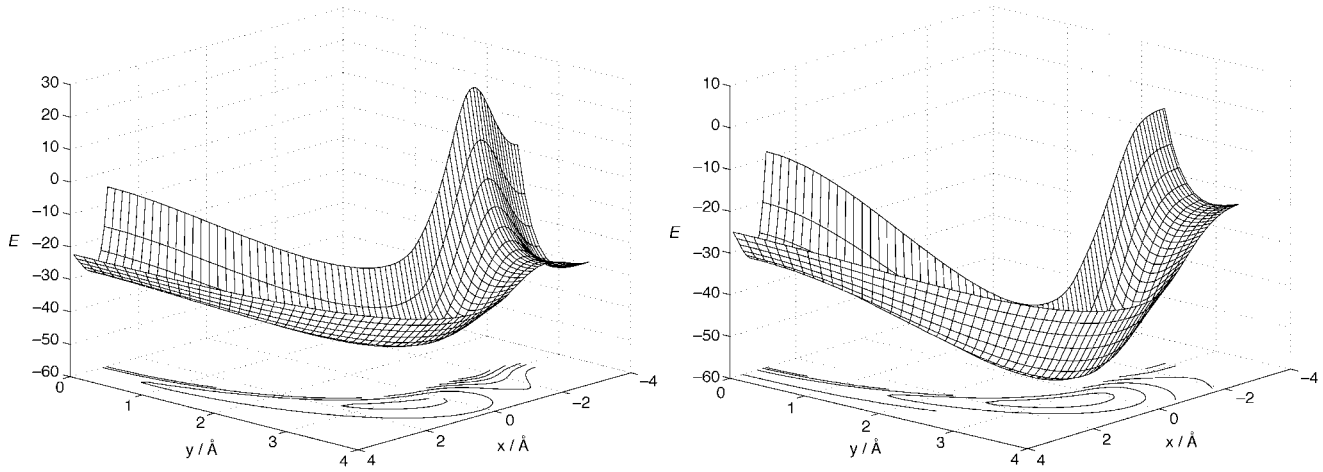

Figure 1. Counterpoise-corrected PES of $I_3^- \cdots I_2$ (left) and $[AuI_2]^- \cdots I_2$ (right). The energy E is given in kJ mol^{-1}.

to an I^- ion. The I–I distances are 2.877 and 3.108 Å and the top angle is 105°, which is in rather good agreement with the experimental values of 2.792 Å, 3.210 Å and 92°.[14] The corresponding calculations for $[AuI_2]^-$ and $[AuI_4]^-$ (D_{4h}) give Au–I distances of 2.661 and 2.722 Å, respectively. These are also slightly too long compared with the average experimental value of 2.566 and 2.626 Å.[14, 19] However, the results are considered acceptable in view of the results for I_3^- and I_5^-.

When the energies for $[AuI_4]^-$ and I_5^- are compared it becomes clear that the square-planar geometry, according to these calculations, is not the most stable one in either case. In both systems, the L-shaped geometry has a lower energy: 58.6 kJ mol^{-1} and 75.8 kJ mol^{-1} lower than for square-planar geometry for $[AuI_4]^-$ and I_5^-, respectively. In the case of I_5^- an even lower total energy can be obtained by allowing the ion to relax to the V-shaped geometry discussed above, but this conformation is only favoured by 3.9 kJ mol^{-1} compared with the L-shaped one. However, the difference in energy between different geometries is small in both systems and in the same order of magnitude as hydrogen bonds (10–65 kJ mol^{-1}). Despite all this, it is interesting to note that the angles in the two L-shaped ions $[AuI_4]^-$ and I_5^- are almost identical, and that the only significant difference is the length of the linear part (the terminal I–I distance in $[AuI_4]^-$ is 5.312 Å and 5.940 Å in I_3^-) of the compounds.

The PES of I_3^- and I_2, (Figure 1 left) shows two minima; one which corresponds to the L-shaped geometry described above and the other to T-shaped. This is surprising since no discrete T-shaped polyiodide structure has been reported so far. However, basis set superposition errors (BSSE) contribute significantly to the energy in the range studied, and the largest contribution, and thereby the largest error, is obtained for the T-shaped structure. The energy difference between the L-shaped and the T-shaped geometry is significant, and larger when corrected for BSSE. The relative difference in energy might explain why only L-shaped I_5^- ions are observed experimentally. However, in solid triiodide compounds the triiodide ions often form T-shaped aggregates and networks.[1–3]

The corresponding PES of $[AuI_2]^-$ and I_2 (Figure 1 right) only displays one minimum which corresponds to the bent L-shape. This indicates that it ought to be possible to use $[AuI_2]^-$ to replace I_3^- in polyiodides, or vice versa in gold(I) compounds which contain $[AuX_2]^-$. We were not able to retain gold in oxidation state +I in the systems studied (see Experimental Section). The high I_2 activity required during synthesis causes the gold to oxidise to +III forming square-planar $[AuI_4]^-$ complexes that are coordinated by excess I_2.

An interesting analogy to the $[I\text{-}I\text{-}I]^-$/$[I\text{-}Au\text{-}I]^-$ systems investigated here is the theoretical study by Hoffman et al. on the $[I\text{-}I\text{-}I]^-$/$[I\text{-}H\text{-}I]^-$/$[I\text{-}I\text{-}H]^-$ systems.[20] They show that $[I\text{-}H\text{-}I]^-$ is favoured over the formation of $[I\text{-}I\text{-}H]^-$ and that the bonding in the hydrogen bihalides can be described as a donor–acceptor interaction between closed-shell fragments, in accordance with the bonding in I_3^-.

Abstract in Swedish: *Polyjodider av den formella sammansättningen $(R_3S)I_x$, där R är en alkylgrupp, bildar smältor vid rumstemperatur. Denna typ av system har visat sig vara lämpliga media för syntes av modifierade polyjodider med komplexa metalljodider. I dessa reaktioner utsätts metalljodiderna I^- och I_3^- för en konkurrens om elektronacceptorn I_2. Detta möjliggör inkorporering av gästmolekyler i polyjodidnätverken. Teoretiska beräkningar har visat att I_5^- och $[AuI_4]^-$ är mycket lika och potentialenergiytan för interaktionen mellan $[MI_2]^-$ och I_2, där M är I eller Au, i båda systemen uppvisar ett minimmum som motsvarar en L-formad struktur. Resultaten av de teoretiska beräkningarna antyder att I_3^- och $[AuI_2]^-$ borde vara utbytbara i fasta strukturer. Dessa resultat stöds av det faktum att föreningarna $(Et_3S)[AuI_4]\cdot 2I_2$, (**1**) och $(Me_3S)_2[AuI_4][I_3]$, (**4**) kan syntetiseras. Föreningarna har karakteriserats med hjälp av röntgendiffraktion, samt Raman- och IR-spektroskopi. Strukturen av **1** innehåller oändliga zigzagkedjor av $[AuI_4]^-$ koordinerad av I_2 i cis-konformation, dvs över AuI_2-diagonalen. $[AuI_4]^-$-enheterna kan därför anses vara en del av ett polyjodid-nätverk. Strukturen av **4** är närbesläktad med den i $M_2Au_2X_6$ (M = vanligen alkalimetallkatjon; X = halogenidjon), vilken består av plankvadratiska $[AuX_4]^-$- och linjära $[AuX_2]^-$-joner. I strukturen av **4** har emellertid $[AuX_2]^-$ ersatts med I_3^-.*

  0947-6539/99/0501-0306 $ 17.50+.50/0 *Chem. Eur. J.* **1999**, *5*, No. 1

A comparison between the two PES shows that the interaction between $[AuI_2]^-$ and I_2 is significantly stronger than the one between I_3^- and I_2; $I_3^- \cdots I_2$ has a more flat potential surface than $[AuI_2]^- \cdots I_2$. Therefore, the potential energy surface for the pure polyiodide is more affected by BSSE and the interaction energy is decreased by 20% at the L-shaped minimum after counterpoise correction, compared with a modest change of 7% for the PES of $AuI_2 \cdots I_2$. Thus, the calculations show that $[AuI_2]^-$ and I_3^-, and $[AuI_4]^-$ and I_5^- are closely related and indicate that both complex $[AuI_2]^-$ and $[AuI_4]^-$ ions are suitable candidates as guest molecule in polyiodide networks.

Structural and spectroscopic investigations: A first attempt to insert complex gold iodides into polyiodides was made by the electrolysis of gold in $(Et_3S)I_5$. The reaction resulted in $(Et_3S)[AuI_4] \cdot 2I_2$ (**1**) which consists of square-planar $[AuI_4]^-$ complexes perpendicularly linked by iodine in the crystallographic *b* direction (Figure 2). The Au–I distances range from 2.62 to 2.64 Å and the I-Au-I angles from 89.5 to 90.5° (Table 1). A comparison with the corresponding iodine-free compound $(Et_3S)[AuI_4]$ (**2**) shows no significant difference in the $[AuI_4]^-$ ion (Au–I 2.62–2.64 Å and I-Au-I 89.7–90.3°) (Figure 3). The average Au–I bond length in **1** (2.64 Å) is slightly longer than in **2** (2.63 Å) although the difference lies within experimental error.

The intramolecular I–I distances in the I_2 molecules are 2.733(2) and 2.738(2) Å, which indicates a significant degree of interaction with the $[AuI_4]^-$ donors (compared with pure I_2 in the solid state, 2.715(6) Å,[21] and gas phase, 2.667(2) Å[22]). The intermolecular I–I distances are typical for those in pure polyiodides, and I–I distances shorter than 3.70 Å have been interpreted in terms of secondary bonds [23] (van der Waals radius of neutral iodine, 2.15 Å). The bridging iodine molecules can thus be regarded as a part of an I_4^{2-} ion and in **1** they form two types of infinite zig-zag chains (Figure 4) in the crystallographic *b* direction. The first chain, which contains Au(1), has intermolecular I–I distances of 3.334(2) and 3.620(2) Å (I(2)–I(6) and I(1)–I(5)) and angles of 170.83(6) and 172.53(6)° (I(6)-I(5)-I(1) and I(5)-I(6)-I(2)). The second chain has intermolecular I–I distances of 3.395(2) and 3.500(2) Å (I(4)–I(8) and I(3)–I(7)) and angles of 173.44(6) and 175.43(6)° (I(7)-I(8)-I(4) and I(8)-I(7)-I(3)).

Table 1. Selected bond lengths [Å] and angles [°] in **1**–**4**.

$(Et_3S)[AuI_4] \cdot 2I_2$ **1**		$(Et_3S)[AuI_4]$ **2**	
Au(1)–I(1)	2.636(1)	Au(1)–I(1)	2.637(2)
Au(1)–I(2)	2.629(2)	Au(1)–I(2)	2.616(1)
Au(2)–I(3)	2.624(2)	Au(2)–I(3)	2.620(1)
Au(2)–I(4)	2.628(2)	Au(2)–I(4)	2.624(2)
I(1)–I(5)	3.620(2)	I(1)-Au(1)-I(2)	90.29(4)
I(2)–I(6)	3.334(2)	I(1)-Au(1)-I(2)	89.71(4)
I(5)–I(6)	2.733(2)	I(3)-Au(2)-I(4)	90.28(5)
I(4)–I(8)	3.395(2)	I(3)-Au(2)-I(4)	89.72(5)
I(3)–I(7)	3.500(2)		
I(7)–I(8)	2.738(2)	$(Et_3S)[AuI_2]$ **3**	
I(1)-Au(1)-I(1)	180.0	Au(1)–I(1)	2.570(4)
I(1)-Au(1)-I(2)	90.47(5)	Au(2)–I(2)	2.554(4)
I(1)-Au(1)-I(2)	89.53(5)	Au(2)–I(3)	2.551(5)
I(3)-Au(1)-I(3)	180	I(1)-Au(1)-I(1)	180
I(4)-Au(1)-I(4)	180	I(2)-Au(2)-I(3)	176.1(2)
I(3)-Au(1)-I(4)	90		
I(6)-I(5)-I(1)	170.83(6)	$(Me_3S)_2[AuI_4][I_3]$ **4**	
I(5)-I(6)-I(2)	172.53(6)	Au–I(2)	2.6298(7)
I(7)-I(8)-I(4)	173.44(6)	Au–I(1)	2.6316(7)
I(8)-I(7)-I(3)	175.43(6)	I(3)–I(4)	2.905(1)
		I(1)-Au(1)-I(2)	90.19(2)
		I(1)-Au(1)-I(2)	89.81(2)

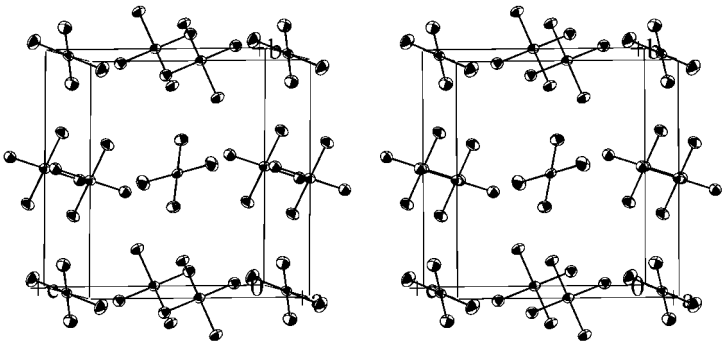

Figure 3. Stereoscopic view of the crystal structure of $(Et_3S)[AuI_4]$. The cations are omitted for clarity.

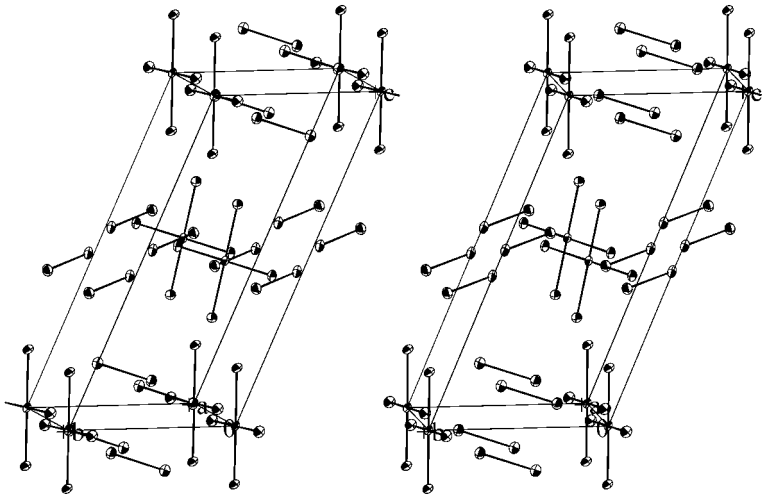

Figure 2. Stereoscopic view of the crystal structure of $(Et_3S)[AuI_4] \cdot 2I_2$. The cations are omitted for clarity.

The Raman spectrum of **1** (Figure 5) shows spectral features at 101 and 127, 146 and 161 cm^{-1} whilst Raman spectrum of the I_2-free compound **2** only displays peaks at 126 and 144 cm^{-1}. Consequently, the peaks of **1** at 127 and 146 cm^{-1} can be assigned to modes that originate from square planar $[AuI_4]^-$. Theoretical calculations confirm that these peaks are $[AuI_4]^-$ modes and are assigned to the ν_2 and ν_1 modes, respectively. The few references available report ν_1 at 148 cm^{-1} and ν_2 at 110 cm^{-1}; thus the peak at 127 cm^{-1} deviates.[24] The peak at 161 cm^{-1}

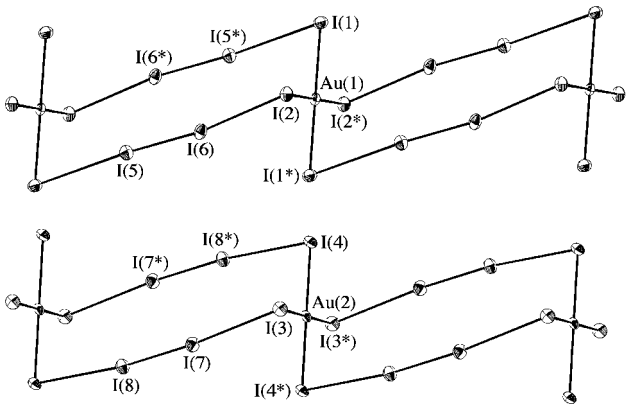

Figure 4. The infinite zigzag chains in $(Et_3S)[AuI_4]\cdot 2I_2$. Top: The chain which contains Au(1). Bottom: The chain which contains Au(2).

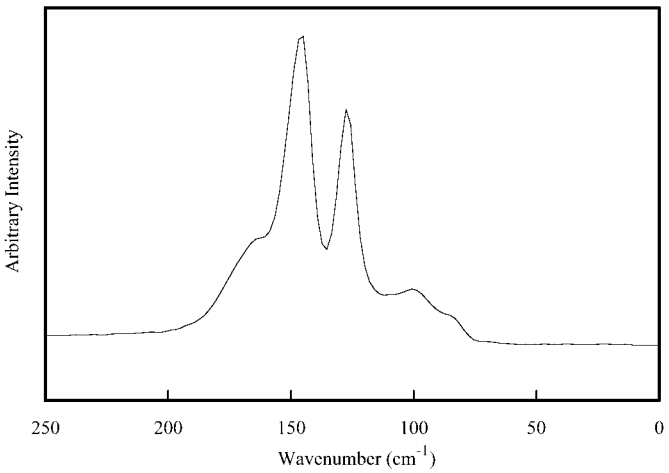

Figure 5. The Raman spectrum of $(Et_3S)[AuI_4]\cdot 2I_2$.

originates from iodine coordinated to $[AuI_4]^-$. Weakly coordinated iodine normally displays a peak at about 180 cm^{-1}.[16–18, 25] Therefore the interaction between the iodine acceptor and the $[AuI_4]^-$ donor can be regarded as fairly strong. The peak at 101 cm^{-1} is more difficult to assign, but a possible explanation is that the IR-active ν_7 mode of $[AuI_4]^-$ has become Raman active because the symmetry has lowered from D_{4h}. Raman and far-IR spectra of the reaction mixtures were also recorded, but because of the strong polyiodide bands the spectra were very difficult to interpret.

Three other binary metal iodide–iodine compounds that form formal tetraiodide bridging units are known in the literature; $(Et_3S)[Hg_2I_6]_{1/2}\cdot 3I_2$, $(Me_3S)[Cd_2I_6]_{1/2}\cdot 3I_2$ and $(NH_4)[AuI_4]\cdot 0.5I_2$.[12, 13, 26] The latter compound consists of almost square planar $[AuI_4]^-$ complexes, where every second complex is coordinated by I_2 molecules, to form a chain structure similar to the one found in **1**. The intra- and intermolecular I–I distances in $(NH_4)[AuI_4]\cdot 0.5I_2$ are 2.709(3) and 3.387(2) Å, respectively. The intramolecular distance indicates a weaker interaction with the gold(III) iodide complex than in **1**, while the intermolecular distances in **1** span a wider range (3.33–3.62 Å). In the cadmium compound, the $[Cd_2I_6]^{2-}$ ions are coordinated by I_2 molecules in such a way that a network of infinite zig-zag chains of $[Cd_2I_6]^{2-}$ complexes interspaced by I_{10} units are formed. The mercury compound also displays a network structure, but in this case the I_2 molecules coordinate directly to the terminal iodine atoms of the $[Hg_2I_6]^{2-}$ ions, and therefore the network becomes less complicated. In both the mercury and cadmium compounds, the intra- and intermolecular I–I distances are similar to those found in **1**.

Efforts were also made to insert $[AuI_2]^-$ and $[AuI_4]^-$ into the polyiodide networks by reaction between Au and $(Et_3S)I_7$ in different solvents (methanol, ethanol, acetonitrile and acetone). However, the reactions gave the non-iodine containing compound $(Et_3S)[AuI_2]$ (**3**), and suitable crystals for structure determination were obtained only from synthesis in methanol. In general, the inclusion of organic solvents during synthesis or at the purification stage (recrystallisation) tends to extract the weakly bound I_2 from the compound. The compound **3** consists of pyramidal Et_3S^+ ions and $[AuI_2]^-$ ions with $D_{\infty h}$ and C_s symmetry (Figure 6). The $[AuI_2]^-$ anions are stacked so that they point to each other to form L- and T-shaped patterns; a structural pattern that is quite common for triiodides.[3, 15, 27] The $[AuI_2]^-$ ion (I(1)-Au(1)-I(1)) with $D_{\infty h}$ symmetry contains an Au–I distance of 2.570(4) Å, while the ion with C_s symmetry (I(2)-Au(2)-I(3)) contains Au–I distances of 2.554(4) and 2.551(5) Å and an angle of 176.1 (2)°. The Au–I distances are in good agreement with those found in the literature.[14, 19]

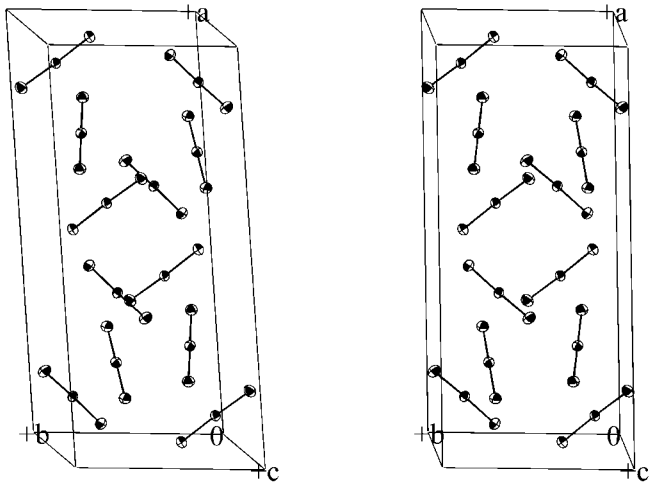

Figure 6. Stereoscopic view of the crystal structure of $(Et_3S)[AuI_2]$. The cations are omitted for clarity.

In another attempt to insert $[AuI_2]^-$ into the polyiodides, the reaction between AuI and $(Me_3S)I_7$ was explored. The cation was changed from triethyl to trimethylsulfonium to facilitate crystallisation. The reaction resulted in black crystals of $(Me_3S)_2[AuI_4][I_3]$ (**4**) (Figure 7) which consists of square planar $[AuI_4]^-$, linear I_3^- and pyramidal Me_3S^+ ions. The I_3^- ion has $D_{\infty h}$ symmetry and the I–I bond length is 2.905(1) Å (I(3)–I(4)) which agrees well with literature data. The $[AuI_4]^-$ ions have Au–I distances of 2.6316(7) (Au–I(1)) and 2.6298(7) Å (Au–I(2)) and I-Au-I angles of 89.81(2) and 90.19(2)°. The I_3^- ions are tilted at an angle of 148.9(3)° ($\measuredangle$ Au···I(4)-I(3)) with respect to the position of gold in $[AuI_4]^-$ (Figure 8) and at a distance of 3.876(1) Å (Au–I(4)). This is

0947-6539/99/0501-0308 $ 17.50+.50/0 *Chem. Eur. J.* **1999**, *5*, No. 1

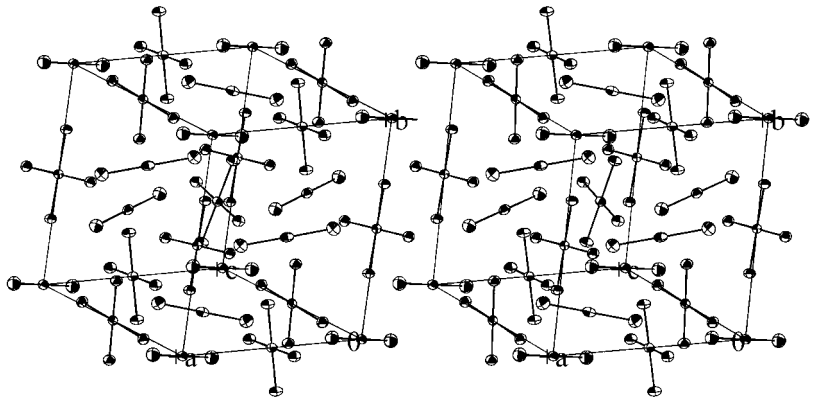

Figure 7. Stereoscopic view of the crystal structure of $(Me_3S)_2[AuI_4][I_3]$. The cations are omitted for clarity.

too long to indicate a direct covalent interaction. However, the partial negative charge on the terminal iodine atoms in I_3^- and the partial positive charge on gold in $[AuI_4]^-$ give rise to a fairly strong electrostatic interaction that may explain the orientation of the I_3^- ions in the structure. It is also notable that the iodine atoms of the $[AuI_4]^-$ ion point towards the central iodine atom of I_3^- in an analogous arrangement.

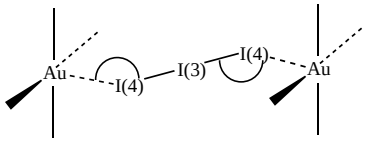

Figure 8. Illustration of the arrangement of I_3^- and $[AuI_4]^-$ in $(Me_3S)_2[AuI_4][I_3]$.

Together with the terminal iodides of the triiodide ions, the square planar $[AuI_4]^-$ ions form chains of elongated octahedra (Figure 9). The gold atoms and the central iodides of the I_3^- ions are positioned in the centres of the octahedra and they alternate to occupy the octahedra in all directions. Since the triiodides are tilted with respect to the $[AuI_4]^-$ plane, the octahedra become quite distorted. However, since all corners of the octahedra are shared, the structure clearly has a perovskite-like appearance. The structure of **4** is quite unique, since there is no other compound in the literature which consists of discrete polyiodide and tetraiodoaurate(III) units. To our knowledge, a few other compounds exist with discrete triiodide ions and metal iodide complexes, but they show no similarities with **4**.[28–31] However, the structure of **4** is similar to the compounds of the $M_2Au_2X_6$ family ($M = Cs^+$, Rb^+, NH_4^+, K^+; $X = Cl^-$, Br^-, I^-) which consist of square-planar $[AuX_4]^-$ and linear $[AuX_2]^-$ ions, instead of the I_3^- ions in **4**.[32, 33] The only compound that has been structurally characterised in this family with $X = I$ is $K_2Au_2I_6$. It contains $[AuI_2]^-$ ions pointing straight towards the equatorial gold atom of the $[AuI_4]^-$ ions instead of the tilted arrangement observed in **4**. However, the structure of $Cs_2Au_2Br_6$ contains $[AuBr_2]^-$ ions tilted in a similar way to the I_3^- ions in **4**. Consequently, the I_3^- ion can be regarded as having substituted the $[AuX_2]^-$ ion in a $M_2Au_2X_6$ structure. It is noteworthy that the $M_2Au_2X_6$ compounds also adopt the perskovite structure.

The results of spectroscopic investigations of **4** support the results obtained from the structural investigation. The Raman spectrum (Figure 10) shows three strong peaks at 147, 130 and

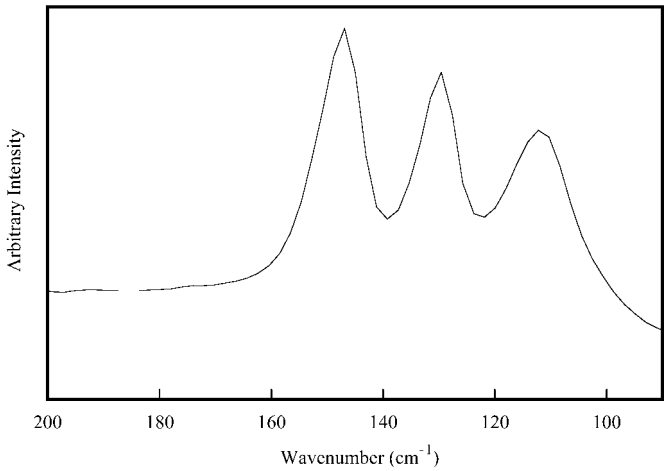

Figure 10. The Raman spectrum of $(Me_3S)_2[AuI_4][I_3]$.

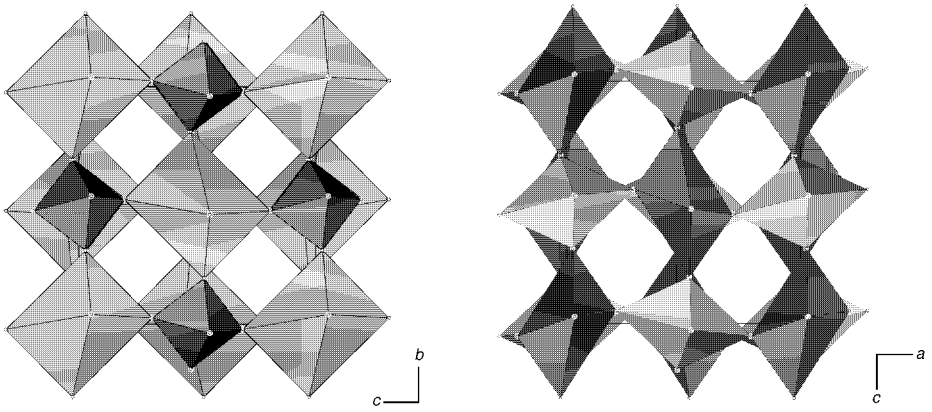

Figure 9. The packing of the MI_6 ($M = Au, I$) octahedra in $(Me_3S)_2[AuI_4][I_3]$.

112 cm^{-1}. The two former peaks are in good agreement with the ν_1 and ν_2 modes of $[AuI_4]^-$ (see data for **1** and **2**). The peak at 112 cm^{-1} is characteristic for the symmetric stretching ν_1 mode of the triiodide ion. The far-IR spectra have peaks at 62, 72, 101, 130, 191 and 205 cm^{-1}. The peaks at 101 and 191 cm^{-1} originate from the ν_7 and ν_6 modes of $[AuI_4]^-$, while the peak at 130 cm^{-1} corresponds to the asymmetric stretching ν_3 mode of I_3^-. The peaks at 62 and

72 cm^{-1} are difficult to assign, since both the I_3^- and $[AuI_4]^-$ ions have modes with frequencies in this region. The weak peak at 205 cm^{-1} is probably the first overtone of the ν_7 mode of $[AuI_4]^-$.

Conclusions

This work has shown that the addition of complex gold iodides to $(R_3S)I_x$ polyiodides identifies a promising route for the modification and investigation of polyiodide networks. The theoretical calculations performed show that $[AuI_4]^-$ and I_5^-, and $[AuI_2]^-$ and I_3^- are closely related and that they are more or less exchangeable, and thus form the basis of a new type of host–guest chemistry. These objectives were verified by the syntheses of the compounds $(Me_3S)_2[AuI_4][I_3]$ and $(Et_3S)[AuI_4]\cdot 2I_2$. The ultimate goal is to obtain a toolbox of additives to modify polyiodide structures in a controlled way and thus be able to design inorganic polymers with specific and low-dimensional physical properties.

Experimental Section

$(Et_3S)[AuI_4]\cdot 2I_2$ (1): Anodical oxidation of gold in a mixture of $(Et_3S)I_5$ in acetonitrile resulted in the formation of **1**. A platinum wire was used as the cathode. Both electrodes were cleaned before use with a warm solution of 1:1 distilled water and concentrated HNO_3. The mass of the gold electrode decreased by 163.46 mg (0.83 mmol) during electrolysis. In the process, 30 equivalents of electrons passed through the system, which shows that the system is more appropriate as a conductor than as a medium for electrolysis. The approximate current used was 10 mA and the applied voltage about 15 V. The yield was estimated to be about 40 % (with respect to Au). $(Et_3S)I_5$ was made by the reaction of $(Et_3S)I$ and I_2 (1:2 molar ratio).
$(Et_3S)[AuI_4]$ (2): Gold pellets (0.632 g, 3.21 mmol) were partly dissolved in a melt of $(Et_3S)I$ (0.811 g, 3.29 mmol) and I_2 (1.244 g, 4.90 mmol) at 90 °C. The reaction mixture was left for two weeks, after which a small sample was allowed to crystallise in methanol. The crystals obtained were red. The yield was estimated to be about 50 % (with respect to Au).

$(Et_3S)[AuI_2]$ (3): A granule of gold (0.277 g, 1.41 mmol) was partly dissolved in a solution of $(Et_3S)I$ (0.409 g, 1.66 mmol) and I_2 (0.207 g, 0.82 mmol) in methanol. This mixture was then refluxed for four days, after which a brown solution and some solid gold remained. The solution was then cooled, which led to the precipitation of dark crystals. The yield was estimated to be about 40 % (with respect to Au).

$(Me_3S)_2[AuI_4][I_3]$ (4): AuI was dissolved in liquid $(Me_3S)I_7$ at 140 °C (molar ratio 1:1). After the reaction mixture cooled to room temperature, acetone was added and the mixture was stored at −30 °C. After several weeks black pyramidal crystals of **4** were obtained. The yield was estimated to be about 60 % (with respect to Au). Free iodine in the gold(I) iodide was removed by evaporation before use. $(Me_3S)I_7$ was made from the reaction of $(Me_3S)I$ and I_2 (1:3 molar ratio).

Vibrational spectroscopy: The far-infrared (far-IR) spectra of the reaction mixtures were recorded on a Bio-Rad FTS 6000 FT-IR spectrometer at a resolution of 8 cm^{-1}. A Globular light source was used, and a 6.25 μm Mylar beamsplitter in combination with a PE-DTGS detector produced an effective spectrum range of 50–550 cm^{-1}. The window material of the sample cells was spectroscopic quality polyethylene (Merck). The back-scattering of the compounds was recorded with 1064 nm radiation from a Nd:YAG laser in a Bio-Rad FT-Raman spectrometer. The radiation was recorded with nitrogen-cooled, Ge-diode detector and at 4 cm^{-1} resolution.

Computational details: The calculations were performed with the GAUSSIAN94 program.[34] Efficiency considerations made it necessary to truncate and contract basis sets available from the literature (Au (5s3p3d)/[221/21/21] and I (5s5d1d)/[221/221/1]).[35] The Stuttgart effective core potentials were used in the calculations.[35] Counterpoise corrections were made for the PES of $I_3^- \cdots I_2$ and $[AuI_2]^- \cdots I_2$ in order to estimate the basis set superposition errors (BSSE).[36]

Geometry optimisations were made for the corresponding gold/iodine compounds $[AuI_2]^-/I_3^-$ and $[AuI_4]^-/I_5^-$. These calculations were made at the HF and MP2 levels. The vibrational frequencies were also calculated in order to verify that the geometries obtained correspond to true minima, and to provide data for comparison with experimental vibrational spectra. When the PES were calculated, both the distance between I_2 and I_3^- (or $[AuI_2]^-$) and the position of I_2 were varied (Figure 11).

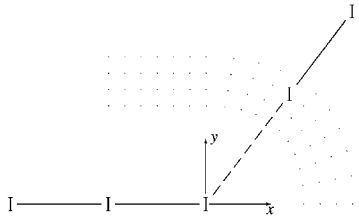

Figure 11. The variation of the position of I_2 in order to estimate the PES for $I_3^- \cdots I_2$ and $[AuI_2]^- \cdots I_2$.

X-ray crystallography: Single crystals of **1** were obtained from the reaction mixture after evaporation of the solvent at room temperature, while crystals of **2**, **3** and **4** were obtained after slow solvent evaporation at −30 °C. The crystallographic data for the structures are presented in Table 2. Data for **1**, **2** and **3** were collected at 150 K on a Enraf-Nonius CAD-4 diffractometer with $Mo_{K\alpha}$ radiation. The data for **4** was collected at room temperature on a Siemens SMART CCD diffractometer. The crystals of **3** were sensitive to X-rays and therefore was the data obtained not of the best quality. The ψ-scan (**1**, **2** and **3**) and SADABS (**4**) methods were used to correct for absorption effects.[37, 38] The structures were solved by the direct methods by using the SIR92 (**1**, **2** and **3**) and SHELXTL-PLUS (**4**) program packages.[39, 40] The structures of **1**, **2** and **3** were refined against *F*, while the structure of **4** was refined against F^2.[41, 40] The unit cell of compound **3** can be reduced to a monoclinic *I* centred cell ($a = 15.31$, $b = 11.10$, $c = 22.65$ Å, $\beta = 91.0°$ and $V = 3848$ Å^3) and the structure can be solved in the space group *I*2/*a*. However, since this is a non-standard setting and the volume is the same in both cell options, the original unit cell was retained even though the β angle is large. The carbon atoms C(3) and C(4) of **1** were refined isotropically due to the high thermal displacement. The carbon atoms closest to the sulfur atom in the cation of compound **2** exhibit disorder over two distinct positions. Because of the severe disorder of the cation in **3**, only one ethyl group was located (refined isotropically). However, the presence of the Et_3S^+ ion in **3** was confirmed by spectroscopic methods. The carbon atoms of the cation in **4** were refined isotropically due to the high thermal displacement and the positional disorder over two sites of the sulfur atom of the cation. Hydrogen atoms were placed in calculated positions in **1**, but omitted in **2**, **3** and **4** because of cation disorder.

Crystallographic data (excluding structure factors) for the structures reported in this paper have been deposited with the Cambridge Crystallographic Data Centre as supplementary publication nos CCDC-102 965 to CCDC-102 968. Copies of the data can be obtained free of charge on application to CCDC, 12 Union Road, Cambridge CB2 1EZ, UK (fax: (+44) 1223-336-033; e-mail: deposit@ccdc.cam.ac.uk).

Acknowledgements

The Swedish Natural Science Research Council and Human Capital & Mobility (contract no. CHRX CT93 0277) are gratefully acknowledged for their financial support.

[1] P. Coppens in *Extended Linear Chain Compounds, Vol. 1* (Ed.: J. S. Miller), Plenum Press, New York, **1982**, p. 333.
[2] T. J. Marks, D. W. Kalina in *Extended Linear Chain Compounds, Vol. 1* (Ed.: J. S. Miller), Plenum Press, New York, **1982**, p. 197.

  0947-6539/99/0501-0310 $ 17.50+.50/0 *Chem. Eur. J.* **1999**, *5*, No. 1

Table 2. Crystallographic data for **1**–**4**.

	1	**2**	**3**	**4**
formula	$C_6H_{15}AuI_8S$	$C_6H_{15}AuI_4S$	$C_6H_{15}AuI_2S$	$C_6H_{18}AuI_7S_2$
M_r	1331.45	823.83	570.02	1239.59
crystal size [mm]	0.10 × 0.10 × 0.15	0.13 × 0.10 × 0.09	0.12 × 0.12 × 0.15	0.28 × 0.35 × 0.15
a [Å]	8.772(3)	7.606(2)	27.11(1)	13.0750(1)
b [Å]	9.450(2)	15.316(3)	11.101(2)	13.4761(1)
c [Å]	16.498(3)	14.275(5)	15.309(4)	13.5150(2)
α [°]	105.07(2)	90	90	90
β [°]	95.25(3)	104.10(3)	123.35(2)	90
γ [°]	115.25(2)	90	90	90
V [Å^3]	1162.0(8)	1612.9(8)	3848(2)	2381.34(4)
Space group	$P\bar{1}$	$P2_1/c$	$C2/c$	$Pbca$
Z	2	4	12	4
ρ_{calcd} [g cm^{-3}]	3.805	3.392	2.873	3.458
μ [cm^{-1}]	170.58	168.90	164.32	154.12
diffractometer	CAD-4	CAD-4	CAD-4	Siemens SMART CCD
radiation	$Mo_{K\alpha}$	$Mo_{K\alpha}$	$Mo_{K\alpha}$	$Mo_{K\alpha}$
scan type	ω-2θ	ω-2θ	ω-2θ	ω
$2\theta_{max}$	50	50	50	56
T [K]	150	150	150	293
total data collected	4359	3191	3721	13472
unique data	4085	3191	3581	2343
R_{int}	0.034	–	0.073	0.0347
observed data	3413 [$I > 3\sigma(I)$]	1683 [$I > 3\sigma(I)$]	1731 [$I > 3\sigma(I)$]	1863 [$I > 2\sigma(I)$]
data/variables	3413/139	1683/95	1731/73	2226/70
goodness of fit	2.38	1.36	3.15	1.07
final difference map	−2.37;2.43	−2.62;1.52	−2.12;5.06	1.67; −2.51
R	4.0	4.2	7.0	4.0[a]
R_w	8.3	4.7	13.4	10.1[b]

[a] $R(F^2)_{obs}$. [b] $R_w(F^2)_{obs}$.

[3] K.-F. Tebbe in *Homoatomic Rings, Chains and Macromoleules of Main-Group Elements* (Ed.: A. L. Rheingold), Elsevier, Amsterdam, **1977**, p. 551.

[4] P. Pyykkö, *Chem. Rev.* **1997**, *97*, 597.

[5] K.-F. Tebbe, R. Buchem, *Angew. Chem.* **1997**, *109*, 1403; K.-F. Tebbe, R. Buchem, *Angew. Chem. Int. Ed. Engl.* **1997**, *37*, 1345.

[6] H. Stegemann, G. Jabs, H. Mittag, L. Schmidt, H. Füllbier, P. Cikmacs, G. Petrovskis, A. Lusis, A. S. Orliukos, *Z. Anorg. Allg. Chem.* **1987**, *555*, 183.

[7] B. B. Owens, B. Pate, P. M. Skarstad, D. L. Worburton, *Solid State Ionics* **1983**, *9/10*, 1241.

[8] E. Falques, P. Molinre, P. Berdahl, T. P. Nguyen, J. Mansot, *Physica C* **1994**, *219*, 297.

[9] W. R. Salaneck, H. R. Thomas, R. W. Bigelow, C. B. Duke, E. W. Plummer, A. J. Heeger, A. G. Macdiarmid, *J. Chem. Phys.* **1980**, *73*, 4746.

[10] A. J. Blake, R. O. Gould, S. Parsons, C. Radek, M. Schröder, *Angew. Chem.* **1995**, *107*, 2563; A. J. Blake, R. O. Gould, S. Parsons, C. Radek, M. Schröder, *Angew. Chem. Int. Ed. Engl.* **1995**, *34*, 237.

[11] A. J. Blake, R. O. Gould, W. S. Li, V. Lippolis, S. Parsons, C. Radek, M. Schröder, *Angew. Chem.* **1998**, *110*, 305; A. J. Blake, R. O. Gould, W. S. Li, V. Lippolis, S. Parsons, C. Radek, M. Schröder, *Angew. Chem. Int. Ed.* **1998**, *37*, 293.

[12] H. Stegemann, K.-F. Tebbe, L. A. Bengtsson, *Z. Anorg. Allg. Chem.* **1995**, *621*, 165.

[13] P. H. Svensson, L. Bengtsson-Kloo, *J. Chem. Soc. Dalton. Trans*, **1998**, 1425.

[14] P. H. Svensson, L. Bengtsson-Kloo, unpublished results.

[15] *Cambridge Structural Database System*, Database V. 5.14, **1997**.

[16] J. Milne, *Spectrochim. Acta* **1992**, *48a*, 553.

[17] P. Deplano, F. A. Devillanova, J. A. Ferraro, F. Isaia, V. Lippolis, M. L. Mercuri, *Appl. Spectrosc.* **1992**, *46*, 1625.

[18] J. S. Zambounis, E. I. Kamitsos, A. P. Patsis, G. C. Papavassiliou, *J. Raman Spectrosc.* **1992**, *23*, 81.

[19] *Inorganic Structural Database ICSD*, V. 5.14, **1997**, Gmelin Institut.

[20] G. A. Landrum, N. Goldberg, R. Hoffman, *J. Chem. Soc. Dalton. Trans.* **1997**, 3605.

[21] F. van Bolhuis, P. B. Koster, T. Migchelsen, *Acta Cryst.* **1967**, *23*, 90.

[22] I. L. Karle, *J. Chem. Phys.* **1955**, *23*, 1739.

[23] M. Bittner, *Präperative und röntgenographische Untersuchungen an Polyiodiden von 2,2′-Bipyridin* , Ph. D. thesis, **1994**, Köln.

[24] P. J. Hendra, *J. Chem. Soc.* **1967**, 1298.

[25] L. Bengtsson, H. Füllbier, B. Holmberg, H. Stegemann, *Molec. Phys.* **1991**, *73*, 283.

[26] E. S. Lang, J. Strähle, *Z. Anorg. Allg. Chem.* **1996**, *622*, 981.

[27] L. A. Bengtsson, Å. Oskarsson, H. Stegemann, A. Redeker, *Inorg. Chem. Acta* **1994**, *215*, 33.

[28] H. Kiriyama, *Cryst. Anal. Res. Cent. Rep* **1983**, 26.

[29] B. Xianhui, P. Coppens, *Acta Cryst.* **1992**, *48*, 1565.

[30] R. Kato, H. Kobayashi, Y. Nishio, K. Kajita, W. Sasaki, *Chem. Lett.* **1986**, 957.

[31] M. A. Beno, U. Geiser, K. L. Kostka, K. S. Webb, M. A. Firestone, K. D. Carlson, L. Nunez, M-H Whangbo, J. M. Williams, *Inorg. Chem.* **1987**, *26*, 1912.

[32] J. Strähle, J. Gelinik, M. Kölmel, *Z. Anorg. Allg. Chem.* **1979**, *456*, 241.

[33] J. Strähle, J. Gelinik, M. Kölmel, A. M. Nemecek, *Z. Naturforsch.* **1979**, *34b*, 1047.

[34] GAUSSIAN94 *(Revision B.3)*, M. J. Frish , G. W. Tucks, H. B. Schlegel, P. M. W. Gill, B. G. Johnson, M. A. Robb, J. R. Cheeseman, T. A. Keith, G. A. Petersson, J. A. Montgomery, K. Raghavachari, M. A. Al-Laham, V. G. Zakrzewski, J. V. Ortiz, J. B. Foresman, J. Cioslowski, B. B. Stafanov, A. Nanayakkara, M. Challacombe, C. Y. Peng, P. Y. Ayala, W. Chen, M. W. Wong, J. L. Andres, E. S. Relogle, R. Gomperts, R. L. Martin, D. J. Fox, J. S. Binkley, D. J. Defrees, J. Baker, J. P. Stewart, M. Head-Gordon, C. Gonzales, J. A. Pople, Gaussian Inc., Pittsburg PA, **1995**.

[35] P. Schwerdtfeger, M. Dolg, W. H. E. Schwarz, G. A. Bowmaker, P. D. Boyd, *J. Chem. Phys.* **1989**, *91*, 1762

[36] F. B. van Duijneveldt, J. G. C. M. van Duijneveldt van de Ridjt, J. H. Lenthe, *Chem. Rev.* **1994**, *94*, 1873.

[37] A. C. T. North, D. C. Phillips, F. S. Mathews, *Acta Cryst. A,* **1968**, *24*, 351.

[38] G. M. Sheldrick, SADABS: Program for Absorption Correction, **1996**, Universität Göttingen, Germany.

[39] A. Altomare, M. C. Burla, M. Camalli, M. Cascarano, C. Giacovazzo, A. Guagliardi, G. Polidori, *J. Appl. Cryst.* **1994**, *27*, 435.

[40] SHELXTL-PLUS, G. M. Sheldrick, Siemens Analytical Instruments, **1992**.

[41] TEXSAN, Crystal Structure Analysis Package, Molecular Structure Corporation **1985**, **1992.**

Received: April 30, 1998 [F 1131]